

# Nonlinear redshift distortions: The two-point correlation function

Somnath Bharadwaj

Department of Physics and Meteorology  
and

Centre for Theoretical Studies  
Indian Institute of Technology  
Kharagpur 721 302 , India

email: somnath@cts.iitkgp.ernet.in

## Abstract

We consider a situation where the density and peculiar velocities in real space are linear, and we calculate  $\xi_s$  the two-point correlation function in redshift space, incorporating all non-linear effects which arise as a consequence of the map from real to redshift space. Our result is non-perturbative and it includes the effects of possible multi-streaming in redshift space. We find that the deviations from the predictions of the linear redshift distortion analysis increase for the higher spherical harmonics of  $\xi_s$ . While the deviations are insignificant for the monopole  $\xi_0$ , the hexadecapole  $\xi_4$  exhibits large deviations from the linear predictions. For a COBE normalised  $\Gamma = 0.25$ ,  $h = 0.5$  CDM power spectrum our results for  $\xi_4$  deviate from the linear predictions by a factor of two at the scales  $\sim 10h^{-1}\text{Mpc}$ . The deviations from the linear predictions depend separately on  $f(\Omega)$  and  $b$ . This holds the possibility of removing the degeneracy that exists between these two parameters in the linear analysis of redshift surveys which yields only  $\beta = f(\Omega)/b$ .

We also show that the commonly used phenomenological model where the non-linear redshift two-point correlation function is calculated by convolving the linear redshift correlation function with an isotropic pair velocity distribution function is a limiting case of our result.

**Keywords:** Cosmology: theory — cosmology: observation — dark matter — galaxies: distances and redshifts — galaxies: clustering — large-scale structure of universe

# 1 Introduction

It has been long recognized that galaxy peculiar motions introduce distortions in the clustering pattern observed in redshift surveys. On small scales, the random motions of galaxies in virialized clusters causes structures to appear elongated along the line of sight, often referred to as the Fingers-of-God. On large scales, the coherent inflow of galaxies into over dense structures causes these to appear flattened along the line of sight (Peebles 1980,§76, and references therein).

In a seminal paper Kaiser (1987) showed that in the linear regime the galaxy peculiar velocities are expected to introduce a quadrupole anisotropy in  $P_s(\mathbf{k})$  the power-spectrum in galaxy redshift surveys, the relation between  $P_s(\mathbf{k})$  and its real space counterpart  $P_r(k)$  being

$$P_s(\mathbf{k}) = (1 + \Omega_0^{0.6} \mu^2)^2 P_r(k) \quad (1)$$

where  $\mu$  is the cosine of the angle between  $\mathbf{k}$  and the line of sight. He proposed that this effect could be used to measure the cosmological density parameter  $\Omega$ . This possibility has led to a lot of work on Linear Redshift Distortions and the reader is referred to Hamilton (1998) for a comprehensive review. Although in principle Kaiser's original proposal is quite simple, there are a large number of problems which arise in the actual analysis of redshift distortions.

One of the main problems arises from the possibility that galaxies may be biased tracers of the underlying mass distribution which determines the peculiar velocities. The fact that galaxies of different types cluster differently (e.g., Dressler 1980; Lahav, Nemiroff & Piran 1990, Santiago & Strauss 1992; Loveday *et al.* 1995; Hermit *et al.* 1996; Guzzo *et al.* 1997) implies that not all of them can be exact indicators of the mass distribution. The presence of bias is a consequence of the complex process of galaxy formation and this suggests a scale dependent, stochastic and nonlinear bias (e.g. Cen & Ostriker 1992, Mann, Peacock & Heavens 1998, Ue-Li Pen 1998, Dekel & Lahav 1999). Various studies (e.g. Taruya *et al.* 2001, Benson *et al.* 2000, Kauffmann, Nusser & Steinmetz 1997) indicate that deterministic linear biasing is a reasonably good assumption at large scales where the density fluctuations are linear. In this situation biasing is described using only one scale independent parameter  $b$  which relates the fluctuation in the galaxy density and the mass density through a linear relation  $\delta_g = b\delta_m$ . It then follows that the analysis of linear redshift distortions allows the determination of the quantity  $\beta = \Omega^{0.6}/b$ , and not  $\Omega$  and  $b$  individually. The analysis of different redshift surveys has given values of  $\beta$  which vary considerably in the range 0.2 – 1.1

(Table. 1 of Hamilton 1998). A part of the large spread in values is related to uncertainties in the nature and extent of bias in the different galaxy samples.

Kaiser's original work and much of the subsequent work is based on the plane-parallel-approximation (PPA) which is valid if the angles subtended by the pairs of galaxies in the analysis are small. The radial nature of the redshift distortions has to be taken into account when analyzing wide angle surveys. Different strategies for incorporating this effect have been studied by Fisher, Scharf & Lahav (1994), Heavens & Taylor (1995), Hamilton & Culhane (1996), Zaroubi & Hoffman (1996), Szalay, Matsubara & Landy (1998) and Bharadwaj (1999). The radial gradients of the galaxy selection function and the motion of the observer introduce new effects when the radial nature of the redshift distortions are taken into account. These two effects do not contribute in the plane parallel approximation.

The linear analysis of redshift distortions, applicable on large scales where the real space density is linear ( $\sigma_l \leq 1$ ), incorporates the distortion due to peculiar velocities only to linear order when transforming from real to redshift space. N-body simulations suggest that non-linear effects are significant in redshift space even at considerably large scales where the real space density field is linear (e.g. Suto & Sugihara 1991; Fisher et al. 1993; Graman, Cen & Bahcall, 1993; Brainerd et al., 1996; Bromley, Warren & Zurek, 1997). This is also seen in the two-point correlation function measured in redshift surveys. In addition to the flattening predicted by the linear analysis, the two-point correlation function remains elongated along the line of sight at scales as large as  $20h^{-1}\text{Mpc}$  (e.g. Figure 2. Peacock *et al.* 2001). This indicates that there is a regime where the density and peculiar velocity fields in real space are adequately described by linear theory, and it is the mapping from real to redshift space which is non-linear. This is often referred to as the translinear regime. It is important to incorporate the non-linear effects in the analysis of redshift distortions in this regime and there have been two different approaches to this problem.

The first approach (e.g. Fisher *et al.* 1994, Peacock & Dodds 1994, Ballinger, Peacock & Heavens 1996) is phenomenological and the effect of the non-linearity is incorporated by convolving the linear redshift two-point correlation function with the line of sight component of a random isotropic pairwise velocity distribution function (eq. 39). Equivalently, these effects are introduced into the power spectrum through a function  $\hat{f}(k, \mu)$  which multiplies the linear redshift power spectrum. The resulting redshift power spectrum is given by

$$P_s(\mathbf{k}) = (1 + \beta\mu^2)^2 P_r(k) \hat{f}(k, \mu). \quad (2)$$

Different forms, including a Gaussian and an exponential, have been used for the distribution function and this approach is found to match the results of N-body simulations well (Hatton & Cole 1998).

The other approach is based on the Zel'dovich approximation. Taylor & Hamilton (1996), Fisher & Nusser (1996) and Hatton and Cole (1998) have used the Zel'dovich approximation to analytically study the behaviour of the redshift-space power spectrum in the translinear regime. They find that the results from Zel'dovich approximation are in agreement with N-body simulations in predicting the shape of the quadrupole to monopole ratio for the redshift power spectrum. They also demonstrate that there can be departures from the linear predictions even at relatively large scales. The first two groups of authors also conclude that the agreement between the Zel'dovich approximation and N-body simulations suggests that it is the coherent infall into over dense structures and not random motions in virialized clusters which is responsible for departures from the linear behaviour in the translinear regime. Recently Hui, Kofman & Shandarin (2000) have used the Zel'dovich approximation to study the probability distribution function of density in redshift space. They find that the peculiar velocities may significantly increase the multi-streaming in redshift space even when this is insignificant in real space. This suggests that non-perturbative effects may be important in the mapping from real to redshift space even when the real space density is relatively linear.

It is the aim of this paper to analytically study the redshift two-point correlation function in the translinear regime focusing on the non-linear effects which arise from the mapping from real to redshift space. It is hoped that such a study will help elucidate the relation between the redshift correlation function and the different real space quantities on which it depends. We consider a situation where the density fluctuations and peculiar velocities are linear in real space, and we calculate  $\xi_s$  the two-point correlation function in redshift space taking into account all non-linear effects of the redshift distortion. The calculation closely follows the method used to calculate the real space two-point correlation function in the Zel'dovich approximation (Bharadwaj 1996b). Our result is non-perturbative and hence it incorporates the effects of multi-streaming in redshift space. Our calculation assumes the plane-parallel approximation and hence the effect of gradients in the selection function and the motion of the observer have been ignored. The calculation is presented in section §2.

In §3 we compare our results with the predictions of linear redshift distortion and investigate the nature and extent of the deviations from the linear results. The effects of linear redshift distortion are quantified by a single

parameter  $\beta = f(\Omega)/b$ , and it is not possible to determine  $\Omega$  and  $b$  separately. We investigate whether this degeneracy is broken and if it becomes possible to determine  $\Omega$  and  $b$  if the non-linear redshift distortions are taken into account.

In §4 we present the summary and discussion.

## 2 Calculating $\xi_s$

The position of a galaxy in redshift space  $\mathbf{s}_1$  differs from its actual position  $\mathbf{r}_1$ , the relation between the two being

$$\mathbf{s}_1 - U_1 \mathbf{n}_1 = \mathbf{r}_1 \quad (3)$$

where  $U_1 = \mathbf{v}_1 \cdot \mathbf{n}_1$  is the line-of-sight component of the peculiar velocity of the galaxy and units have been chosen so that the Hubble parameter  $H = 1$ . We study how the galaxy two-point correlation function in phase space  $\rho_{2r}(\mathbf{r}_1, \mathbf{r}_2, \mathbf{v}_1, \mathbf{v}_2)$  is related to its redshift space counterpart  $\rho_{2s}(\mathbf{s}_1, \mathbf{s}_2, \mathbf{v}_1, \mathbf{v}_2)$ .

The mapping from real space to redshift space preserves the number of galaxies

$$\rho_{2s}(\mathbf{s}_1, \mathbf{s}_2, \mathbf{v}_1, \mathbf{v}_2) d^3 s_1 d^3 s_2 d^3 v_1 d^3 v_2 = \rho_{2r}(\mathbf{r}_1, \mathbf{r}_2, \mathbf{v}_1, \mathbf{v}_2) d^3 r_1 d^3 r_2 d^3 v_1 d^3 v_2 \quad (4)$$

For pairs of galaxies which are at a large distance from the observer and subtends a small angle in the sky, the Jacobian of the transformation from  $\mathbf{s}$  to  $\mathbf{r}$  (eq. 3) may be neglected and we get

$$\rho_{2s}(\mathbf{s}_1, \mathbf{s}_2, \mathbf{v}_1, \mathbf{v}_2) = \rho_{2r}(\mathbf{s}_1 - U_1 \mathbf{n}, \mathbf{s}_2 - U_2 \mathbf{n}, \mathbf{v}_1, \mathbf{v}_2) \quad (5)$$

in the “plane parallel approximation”. Here the unit vector  $\mathbf{n}$  refers to the common line-of-sight to the pair of galaxies, and the line-of-sight components of the peculiar velocity of the two galaxies are taken to be parallel.

The phase space two-point correlation function in real space is homogeneous which allows us to write equation (5) as

$$\rho_{2s}(\mathbf{s}_1, \mathbf{s}_2, \mathbf{v}_1, \mathbf{v}_2) = \rho_{2r}(\mathbf{s} - U \mathbf{n}, \mathbf{v}_1, \mathbf{v}_2) \quad (6)$$

where  $\mathbf{s} = \mathbf{s}_2 - \mathbf{s}_1$  is the vector joining the pair of galaxies and  $U = \mathbf{n} \cdot (\mathbf{v}_2 - \mathbf{v}_1)$  is the line-of-sight component of the difference in peculiar velocities of the two galaxies. The vector  $\mathbf{s}$  is decomposed into two parts

$$\mathbf{s} = \mathbf{s}_\perp + s_\parallel \mathbf{n}, \quad (7)$$

$s_{\parallel}$  the component along the line-of-sight and  $\mathbf{s}_{\perp}$  the part perpendicular to the line-of-sight.

A Taylor expansion of equation (6) in powers of  $U$  gives us

$$\rho_{2s}(\mathbf{s}_1, \mathbf{s}_2, \mathbf{v}_1, \mathbf{v}_2) = \sum_{m=0}^{\infty} \frac{(-U)^m}{m!} \frac{\partial^m}{\partial s_{\parallel}^m} \rho_{2r}(\mathbf{s}, \mathbf{v}_1, \mathbf{v}_2). \quad (8)$$

We calculate  $\xi_s(s_{\perp}, s_{\parallel})$  the galaxy two-point correlation function in redshift space by integrating out the velocity information in equation (8)

$$\begin{aligned} \bar{n}_g^2 [1 + \xi_s(s_{\perp}, s_{\parallel})] &= \int d^3v_1 d^3v_2 \rho_{2s}(\mathbf{s}, \mathbf{v}_1, \mathbf{v}_2) \\ &= \int d^3v_1 d^3v_2 \sum_{m=0}^{\infty} \frac{(-U)^m}{m!} \frac{\partial^m}{\partial s_{\parallel}^m} \rho_{2r}(\mathbf{s}, \mathbf{v}_1, \mathbf{v}_2). \end{aligned} \quad (9)$$

where  $n_g$  is the mean number density of galaxies and  $s_{\perp} = |\mathbf{s}_{\perp}|$ . Equation (9) relates the galaxy two-point correlation in redshift space to a sum of velocity moments of different orders in real space. The velocity moments in real space can also be expressed as

$$\int d^3v_1 d^3v_2 U^m \rho_{2r}(\mathbf{s}, \mathbf{v}_1, \mathbf{v}_2) = \bar{n}_g^2 \langle U^m (1 + \delta_{1r})(1 + \delta_{2r}) \rangle \quad (10)$$

where  $\langle \rangle$  denotes ensemble average, and  $\delta_1$  and  $\delta_2$  refer to the perturbation in the galaxy number density at the position  $\mathbf{s}_1$  and  $\mathbf{s}_2$  in real space. Using this and separating the odd and even powers of  $U$  in equation (9) we obtain

$$\begin{aligned} 1 + \xi_s(s_{\perp}, s_{\parallel}) &= \sum_{q=0}^{\infty} \frac{1}{(2q)!} \left( \frac{\partial}{\partial s_{\parallel}} \right)^{2q} \langle U^{2q} (1 + \delta_{1r})(1 + \delta_{2r}) \rangle \\ &\quad - \sum_{q=0}^{\infty} \frac{1}{(2q+1)!} \left( \frac{\partial}{\partial s_{\parallel}} \right)^{2q+1} \langle U^{2q+1} (1 + \delta_{1r})(1 + \delta_{2r}) \rangle. \end{aligned} \quad (11)$$

Our analysis is restricted to a situation where the peculiar velocities and density perturbations are linear in real space. It is also assumed that these quantities are a Gaussian random field. We next discuss some of the statistical properties of  $U$  and  $\delta$  in real space.

The ensemble average of an odd number of  $U$ 's and  $\delta$ 's is zero. For example

$$\langle U \rangle = \langle \delta_{1r} \rangle = \langle U \delta_{1r} \delta_{2r} \rangle = 0. \quad (12)$$

The quantities in terms of which we express all the velocity moments encountered in equation (9) are the real space galaxy two-point correlation

$$\xi_r(s_{\perp}, s_{\parallel}) = \langle \delta_1 \delta_2 \rangle, \quad (13)$$

the line-of-sight component of the pair velocity

$$V_P(s_\perp, s_\parallel) = \langle U(\delta_1 + \delta_2) \rangle = \mathbf{n} \cdot \langle (\mathbf{v}_2 - \mathbf{v}_1)(\delta_1 + \delta_2) \rangle, \quad (14)$$

and the dispersion of the line-of-sight component of the pair velocity

$$\sigma_P^2(s_\perp, s_\parallel) = \langle U^2 \rangle = \mathbf{n}_i \mathbf{n}_j \langle (\mathbf{v}_2 - \mathbf{v}_1)_i (\mathbf{v}_2 - \mathbf{v}_1)_j \rangle. \quad (15)$$

We also have the relation

$$V_P(s_\perp, s_\parallel) = 2 \langle U \delta_{1r} \rangle = 2 \langle U \delta_{2r} \rangle. \quad (16)$$

which follows from the statistical isotropy and homogeneity of the peculiar velocities and perturbations.

All the higher velocity moments can be expressed in terms of  $\xi_s$ ,  $V_P$  and  $\sigma_P^2$ . In addition, these three quantities are not independent and they can be related using linear perturbation theory (§4).

We first consider the term  $\langle U^{2q} \rangle$  which can be expressed as

$$\langle U^{2q} \rangle = \frac{(2q)!}{2^q q!} [\sigma_P^2(s_\perp, s_\parallel)]^q. \quad (17)$$

We next consider the even velocity moments in equation (11). These can be expressed as (for  $q > 0$ )

$$\begin{aligned} & \langle U^{2q} (1 + \delta_{1r})(1 + \delta_{2r}) \rangle = \\ &= \langle U^{2q} \rangle \langle (1 + \delta_{1r})(1 + \delta_{2r}) \rangle + (2q)(2q-1) \langle U^{2q-2} \rangle \langle U \delta_{1r} \rangle \langle U \delta_{2r} \rangle \\ &= \frac{(2q)!}{2^q q!} [\sigma_P^2(s_\perp, s_\parallel)]^q [1 + \xi_r(s_\perp, s_\parallel)] + \frac{(2q)!}{2^{q-1}(q-1)!} [\sigma_P^2(s_\perp, s_\parallel)]^{q-1} \frac{V_P^2(s_\perp, s_\parallel)}{4}, \end{aligned} \quad (18)$$

and for the odd moments we have

$$\begin{aligned} \langle U^{2q+1} (1 + \delta_{1r})(1 + \delta_{2r}) \rangle &= (2q+1) \langle U^{2q} \rangle \langle U(\delta_{1r} + \delta_{2r}) \rangle \\ &= \frac{(2q+1)!}{2^q q!} [\sigma_P^2(s_\perp, s_\parallel)]^q V_P(s_\perp, s_\parallel). \end{aligned} \quad (19)$$

Using these for the odd and even terms in equation (11) we get

$$\begin{aligned} 1 + \xi_s(s_\perp, s_\parallel) &= \sum_{q=0}^{\infty} \frac{1}{2^q q!} \frac{\partial^{2q}}{\partial s_\parallel^{2q}} \left( [\sigma_P^2(s_\perp, s_\parallel)]^q [1 + \xi_r(s_\perp, s_\parallel)] \right. \\ &\quad \left. - \frac{\partial}{\partial s_\parallel} \{ [\sigma_P^2(s_\perp, s_\parallel)]^q V_P(s_\perp, s_\parallel) \} + \frac{\partial^2}{\partial s_\parallel^2} \{ [\sigma_P^2(s_\perp, s_\parallel)]^q \frac{V_P^2(s_\perp, s_\parallel)}{4} \} \right) \end{aligned} \quad (20)$$

Each of the three terms in the above equation is next expressed using a Dirac Delta function.

$$\delta^3(\mathbf{s} - \mathbf{s}') = \int \frac{d^3 k}{(2\pi)^3} \exp[i(\mathbf{s} - \mathbf{s}') \cdot \mathbf{k}]. \quad (21)$$

Below we show this procedure for the third term in equation (20).

$$\begin{aligned} \frac{\partial^{2q+2}}{\partial s_{\parallel}^{2q+2}} \{ [\sigma_P^2(\mathbf{s})]^q \frac{V_P^2(\mathbf{s}')}{4} \} &= \frac{\partial^{2q+2}}{\partial s_{\parallel}^{2q+2}} \int d^3 s' \delta^3(\mathbf{s} - \mathbf{s}') \{ [\sigma_P^2(\mathbf{s}')]^q \frac{V_P^2(\mathbf{s}')}{4} \} \\ &= \int d^3 s' \frac{V_P^2(\mathbf{s}')}{4} \frac{\partial^2}{\partial s_{\parallel}^2} \int \frac{d^3 k}{(2\pi)^3} \exp[i(\mathbf{s} - \mathbf{s}') \cdot \mathbf{k}] [-k_{\parallel}^2 \sigma_P^2(\mathbf{s}')]^q \end{aligned} \quad (22)$$

where  $k_{\parallel} = \mathbf{k} \cdot \mathbf{n}$  is the line of sight component of  $\mathbf{k}$ .

Carrying out a similar procedure for all the terms in (20) we obtain

$$\begin{aligned} 1 + \xi_s(s_{\perp}, s_{\parallel}) &= \int d^3 s' \left[ \xi_r(s'_{\perp}, s'_{\parallel}) + \left( 1 - \frac{V_P(s'_{\perp}, s'_{\parallel})}{2} \frac{\partial}{\partial s_{\parallel}} \right)^2 \right] \times \\ &\quad \times \int \frac{d^3 k}{(2\pi)^3} \exp[i(\mathbf{s} - \mathbf{s}') \cdot \mathbf{k}] \sum_{q=0}^{\infty} \frac{1}{2^q q!} [-k_{\parallel}^2 \sigma_P^2(s'_{\perp}, s'_{\parallel})]^q \end{aligned} \quad (23)$$

The sum over  $q$  gives a Gaussian in  $k_{\parallel}$  which can be integrated

$$\int \frac{d^3 k}{(2\pi)^3} \exp[i(\mathbf{s} - \mathbf{s}') \cdot \mathbf{k}] \exp \left[ -\frac{k_{\parallel}^2 \sigma_P^2(s'_{\perp}, s'_{\parallel})}{2} \right] = \delta^2(\mathbf{s}_{\perp} - \mathbf{s}'_{\perp}) G(s_{\parallel} - s'_{\parallel}, \sigma_P(s'_{\perp}, s'_{\parallel})), \quad (24)$$

where we use

$$G(x, a) = \frac{1}{\sqrt{2\pi}a} \exp\left[-\frac{x^2}{2a^2}\right] \quad (25)$$

to represent a normalised Gaussian distribution.

Using this in equation (23) we can integrate over  $d^2 s_{\perp}$  to get

$$1 + \xi_s(s_{\perp}, s_{\parallel}) = \int ds'_{\parallel} \left[ \xi_r(s_{\perp}, s'_{\parallel}) + \left( 1 - \frac{V_P(s_{\perp}, s'_{\parallel})}{2} \frac{\partial}{\partial s_{\parallel}} \right)^2 \right] G(s_{\parallel} - s'_{\parallel}, \sigma_P(s_{\perp}, s'_{\parallel})) \quad (26)$$

Replacing  $\partial/\partial s_{\parallel}$  with the derivatives of the Gaussian distribution and making a change of variable  $s'_{\parallel} - s_{\parallel} \rightarrow s'_{\parallel}$  gives us

$$\begin{aligned} 1 + \xi_s(s_{\perp}, s_{\parallel}) &= \int ds'_{\parallel} G(s'_{\parallel}, \sigma_P(s_{\perp}, s_{\parallel} + s'_{\parallel})) \times \\ &\quad \times \left[ \xi_r(s_{\perp}, s_{\parallel} + s'_{\parallel}) + \left( 1 - \frac{s'_{\parallel} V_P(s_{\perp}, s_{\parallel} + s'_{\parallel})}{2\sigma_P^2(s_{\perp}, s_{\parallel} + s'_{\parallel})} \right)^2 - \frac{V_P^2(s_{\perp}, s_{\parallel} + s'_{\parallel})}{4\sigma_P^2(s_{\perp}, s_{\parallel} + s'_{\parallel})} \right]. \end{aligned} \quad (27)$$

This expresses the galaxy two-point correlation function in redshift space as a function of there quantities in real space, namely the galaxy two-point correlation function  $\xi_r$ , the line-of-sight component of the pair velocity  $V_P$  and the dispersion of line-of-sight component of the pair velocity  $\sigma_P^2$ . Equation (27) is non-perturbative and it incorporates all the effects of redshift space distortions. This includes multi-streaming in redshift space and all other non-linear effects which may arise due to the mapping from real to redshift space.

### 3 Comparison with linear results.

Kaiser (1987) and Hamilton (1992) have analyzed the effect of linear redshift distortions on the two-point correlation function. We use  $\xi_s^L$  to refer to this and in this section we compare  $\xi_s^L$  with  $\xi_s$  which incorporates non-linear redshift distortions.

The expression for  $\xi_s^L$  is obtained by keeping only the linear terms in equation (20) which gives

$$\xi_s^L(s_\perp, s_\parallel) = \xi_r(s_\perp, s_\parallel) - \frac{\partial}{\partial s_\parallel} V_P(s_\perp, s_\parallel) + \frac{1}{2} \frac{\partial^2}{\partial s_\parallel^2} \sigma_P^2(s_\perp, s_\parallel) \quad (28)$$

In the linear regime, under the assumption of linear bias, the real space quantities  $\xi_r$ ,  $V_P$  and  $\sigma_P^2$  can be expressed in terms of  $\xi$ , the two-point correlation function of the underlying dark matter distribution (details in Appendix A), as

$$\xi_r(s_\perp, s_\parallel) = b^2 \xi(s) \quad (29)$$

where  $b$  is the linear bias parameter and  $s = \sqrt{s_\perp^2 + s_\parallel^2}$ . We also have

$$V_P(s_\perp, s_\parallel) = -2 f(\Omega) b \frac{\partial}{\partial s_\parallel} (\nabla^2)^{-1} \xi(s) = -\frac{2}{3} s_\parallel f(\Omega) b \bar{\xi}_2(s) \quad (30)$$

and

$$\begin{aligned} \sigma_P^2(s_\perp, s_\parallel) &= 2 \left[ f^2(\Omega) \frac{\partial^2}{\partial s_\parallel^2} (\nabla^2)^{-2} \xi(s) + \sigma^2 \right] \\ &= f^2(\Omega) \left[ \frac{s^2}{3} \bar{\xi}_1(s) - \frac{s_\perp^2}{3} \bar{\xi}_2(s) + \frac{(s^2 - 3s_\parallel^2)}{15} \bar{\xi}_4(s) \right] \end{aligned} \quad (31)$$

where  $f(\Omega) \approx \Omega^{0.6}$  is the dimensionless growth rate for linear perturbation (Peebles 1980),  $\sigma^2$  is the one-dimensional peculiar velocity dispersion and

$$\bar{\xi}_n(s) = \frac{n+1}{s^{n+1}} \int_0^s \xi(y) y^n dy. \quad (32)$$

We use equations (29),(30) and (31) to express both  $\xi_s^L$  (eq. 28) and  $\xi_s$  (eq. 27) in terms of only three inputs namely  $f(\Omega), b$  and  $\xi$ . This gives an operator equation (eq. 4 of Hamilton 1992)

$$\xi_s^L(s_\perp, s_\parallel) = \left[ b + f(\Omega) \frac{\partial^2}{\partial s_\parallel^2} (\nabla^2)^{-1} \right]^2 \xi(s) \quad (33)$$

for the linear redshift two-point correlation  $\xi_s^L$  in terms of  $\xi$  the actual two-point correlation of the underlying dark matter distribution.

An alternative way to parametrize the anisotropy of the redshift two-point correlation function is to use  $s$  and  $\mu = s_\parallel/s$  (the cosine of the angle between  $\mathbf{s}$  and the line of sight  $\mathbf{n}$ ) instead of  $(s_\perp, s_\parallel)$ . The angular dependence of  $\xi_s^L(s, \mu)$  can be very conveniently expressed as a sum of spherical harmonics (Hamilton 1992) as

$$\xi_s^L(s) = \xi_0^L(s) P_0(\mu) + \xi_2^L(s) P_2(\mu) + \xi_4^L(s) P_4(\mu) \quad (34)$$

where  $P_l(\mu)$  are the Legendre Polynomials and  $\xi_0^L, \xi_2^L$  and  $\xi_4^L$  are the monopole, quadrupole and the hexadecapole components of the linear redshift two-point correlation function. In the linear analysis these

$$\xi_0^L(s) = b^2 \left( 1 + \frac{2}{3} \beta + \frac{1}{5} \beta^2 \right) \xi(s) \quad (35)$$

$$\xi_2^L(s) = b^2 \left( \frac{4}{3} \beta + \frac{4}{7} \beta^2 \right) (\xi(s) - \bar{\xi}_2(s)) \quad (36)$$

$$\xi_4^L(s) = \frac{8}{35} \beta^2 b^2 \left[ \xi(s) + \frac{5}{2} \bar{\xi}_2(s) - \frac{7}{2} \bar{\xi}_4(s) \right]; \quad (37)$$

are the only non-zero harmonics, and here  $\beta = f/b$ . The two-point correlation function of the underlying dark matter distribution is largely undetermined and equation (35) cannot be used to determine both  $b$  and  $\beta$ . The ratios of  $\xi_0^L, \xi_2^L$  and  $\xi_4^L$  can be used to only determine  $\beta$ . It is a limitation of the linear analysis that  $b$  and  $f(\Omega)$  cannot be determined individually.

The angular dependence of  $\xi_s(s, \mu)$  can also be expanded in terms of spherical harmonics

$$\xi(s, \mu) = \sum_{l=0}^{l=\infty} \xi_l(s) P_l(\mu). \quad (38)$$

and here, as in the linear analysis, the odd terms are all zero. However in this case there are no simple analytic expressions for the spherical harmonics and these have to numerically evaluated.

We have used a COBE normalised (Bunn and White, 1996) CDM power spectrum (Efstathiou, Bond and White, 1992) with shape parameter  $\Gamma = 0.25$  and  $h = 0.5$  to calculate the real space two-point correlation function for the underlying dark matter distribution. This model predicts  $\sigma_8 = 0.55$  and we expect non-linear effects to be small in real space at scales  $\geq 10 h^{-1}\text{Mpc}$ . Below we compare the spherical harmonics of  $\xi_s(s, \mu)$  and  $\xi_s^L(s, \mu)$  for this model for different values of  $f$  and  $b$ .

We first consider the case  $f = 1, b = 1$  for which the various spherical harmonics are shown in figure 1. We find that the deviations from the linear predictions are more pronounced for the higher spherical harmonics. While the behaviour of the monopole  $\xi_0^L$  shows practically no deviations from  $\xi_0^L$ ,  $\xi_4$  exhibits significant deviations from  $\xi_4^L$ . Another feature is that the non-linear redshift distortions produce a non-zero  $\xi_6$  whereas the linear analysis predicts a value of *zero* for this and all higher harmonics. We have not considered any of the higher harmonics here.

We next analyze the behaviour of  $\xi_2$  and  $\xi_4$  in some more detail using the quantity  $R_l(s) = \xi_l(s)/\xi_l^L(s)$  whose deviation from the value  $R_l(s) = 1$  indicates departures from the linear predictions. The behaviour of  $R_2$  and  $R_4$  are shown in figures 2 and 3. We see that the behaviour of  $R_2$  and  $R_4$  looks similar, the difference being that the magnitude of the deviations from the linear predictions is much larger for the latter. A feature common to  $R_2$  and  $R_4$  is that the deviations from the linear predictions increase monotonically as we go to smaller length-scales for low  $f(\Omega)$ , whereas for larger  $f(\Omega)$  the deviations saturate and even fall at smaller scales. A possible explanation is that at small scales the anisotropies in  $\xi_s$  are erased by multi-streaming in redshift space. The peculiar velocities increase with  $f(\Omega)$  and we can expect the effects of multi-streaming to also increase with  $f(\Omega)$ . We find that  $\xi_4$  is around a factor of two larger than  $\xi_4^L$  on scales  $10 - 20 h^{-1}\text{Mpc}$  where the non-linear effects are expected to be small in real space. The value of  $R_4$  increases at scales smaller than  $10 h^{-1}\text{Mpc}$  but real space non-linear effects are also expected to become significant at these scales and our results are not expected to give the true picture here. Both  $R_2$  and  $R_4$  approach one at large scales.

The  $b$  and  $f(\Omega)$  dependence of the non-linear redshift space distortions cannot be expressed through just one parameter  $\beta$ . We consider the behaviour of the ratio  $\xi_4(s)/\xi_0(s)$  (figure 4) to study this effect. Linear redshift distortions (eqs. 35 and 37) predict this to depend on just  $\beta$ . We see that

the our predictions for  $\xi_4(s)/\xi_0(s)$  change considerably if we vary  $f(\Omega)$  and  $b$  keeping  $\beta$  fixed. This holds the possibility of using the redshift two-point correlation function to determine  $f(\Omega)$  and  $b$  separately.

## 4 Discussion and summary.

We have calculated  $\xi_s$  the galaxy two-point correlation function in redshift space for a situation where the density fluctuations and peculiar velocities are linear in real space. Our calculation incorporates all non-linear effects which arise due to the mapping from real to redshift space. Our result (equation 27) is non-perturbative and it includes the effects of multi-streaming in redshift space.

The position of a galaxy in redshift space is a combination of its actual position and the line of sight component of its peculiar velocity, and the redshift two-point correlation function will have contributions from three effects

1. Correlations between the actual positions of the galaxies. This is quantified by the real space two-point correlation  $\xi_r(s)$ .
2. Correlations between the peculiar velocities and the actual positions of galaxies. This is quantified by the mean pair velocity whose component along the light of sight is  $V_P(\mathbf{s})$ . In the linear regime this is negative (eq 45) because of coherent flows out of under dense regions and into over dense regions.
3. Correlations between the peculiar velocities of galaxies. This is quantified by the pair velocity dispersion whose component along the light of sight is  $\sigma_P^2(\mathbf{s}) = 2[\sigma^2 - \langle \mathbf{n} \cdot \mathbf{v}(\mathbf{s}_1) \mathbf{n} \cdot \mathbf{v}(\mathbf{s}_2) \rangle]$  where  $\mathbf{s} = \mathbf{s}_2 - \mathbf{s}_1$ . Here  $\sigma^2$  is the one dimensional peculiar velocity dispersion of the random motion of individual galaxies and  $\langle \mathbf{n} \cdot \mathbf{v}(\mathbf{s}_1) \mathbf{n} \cdot \mathbf{v}(\mathbf{s}_2) \rangle = -f^2 \frac{\partial^2}{\partial s_{\parallel}^2} (\nabla^2)^{-2} \xi(s)$  (eq. 47) is the correlation in the line of sight component of peculiar velocities due to coherent flows. At large separations the effect of the coherent flows is much smaller than the contribution from random motions and  $\sigma_P^2(\mathbf{s}) \simeq 2\sigma^2$ . The velocity-velocity correlations due to coherent flows increases at smaller separations. This causes  $\sigma_P^2(\mathbf{s})$  to be anisotropic and its value is less than  $2\sigma^2$ . In the linear analysis  $\sigma_P^2(\mathbf{s})$  decreases monotonically as  $s$  is reduced and  $\sigma_P^2(0) = 0$ .

The linear redshift two-point correlation (eq. 28) incorporates these three effects and  $\xi_s^L(\mathbf{s})$  at a separation  $\mathbf{s}$  in redshift space is expressed in terms of

$\xi_r(\mathbf{s})$ ,  $V_P(\mathbf{s})$  and  $\sigma_P^2(\mathbf{s})$  at the same separation in real space. The line of sight component of the relative peculiar velocity  $U$  between a pair of galaxies causes their separation in redshift space to be different from the actual separation, and in principle the real space quantities should be evaluated at a different separation  $\mathbf{r}$  where  $r_{\parallel} = s_{\parallel} - U$  and  $r_{\perp} = s_{\perp}$ . A possible way to incorporate this effect is to use (eq. 28) for  $\xi_s^L(\mathbf{s})$  and evaluate all the real space quantities at  $\mathbf{r}$ , assuming that the different values of  $U$  being given by a probability distribution  $f(U)$ . This gives

$$\xi_s(s_{\perp}, s_{\parallel}) = \int dU f(U) \xi_s^L(s_{\perp}, s_{\parallel} - U). \quad (39)$$

The distribution of  $U$  is characterized by  $\sigma_P^2(s_{\perp}, s_{\parallel})$  which in general is anisotropic and scale dependent. As a simplifying assumption the distribution of  $U$  is usually taken to be isotropic and the function  $f(U)$  is chosen to be either a Gaussian or an exponential with only one constant parameter  $2\sigma^2$  which is the value of  $\sigma_P^2(\mathbf{s})$  at large separations. This phenomenological model for the non-linear redshift two-point correlation has been found to match the results of N-body simulations. Two effects which are not included in this model are (1.) the anisotropy and spatial dependence of  $\sigma_P^2(\mathbf{s})$  arising from the coherent flows, and (2.) the fact that the distribution of  $U$  is correlated with the density fluctuations.

Our exact calculation takes into account all of the effects discussed above. We find that the redshift two-point correlation function (eq. 27) can be expressed as the real space two-point correlation function combined with ratios of the pair velocity to the pair velocity dispersion, convolved along the line of sight with a Gaussian one dimensional pair velocity distribution. To get a better understanding of the various terms in (eq. 27) we first consider a limiting situation where the separation  $s$  is taken to be large so that  $\langle \mathbf{n} \cdot \mathbf{v}(\mathbf{s}_1) \mathbf{n} \cdot \mathbf{v}(\mathbf{s}_2) \rangle \ll \sigma^2$  i.e. the contribution to  $\sigma_P^2(\mathbf{s})$  from the random motions is much larger than the contribution from coherent flows. In this situation we can ignore the spatial variation of  $\sigma_P^2(\mathbf{s})$  (except for the contribution of the derivative of  $\sigma_P^2(\mathbf{s})$  to  $\xi_s^L(\mathbf{s})$ ). The calculation of  $\xi_s$  in this limit is presented in Appendix B. We find that in this limit the result of our calculation (eq. 51) is identical to the phenomenological model (eq. 39) with a Gaussian pair velocity distribution. This can be interpreted in terms of a simple picture where all the non-linear effects of the redshift distortions on  $\xi_s$  arise from the random motions of galaxies. The random rearrangement of the galaxy positions over the length scale  $\sigma$  along the line of sight in redshift surveys modulates the linear redshift correlation function  $\xi_s^L(s)$ . This diffusion process acting on  $\xi_s^L(\mathbf{s})$  along the line of sight introduces

an elongation in  $\xi_s$ .

It is interesting to note that a similar interpretation is also possible for the non-linear effects on the two-point correlation function in the Zel'dovich approximation (Bharadwaj 1996b) and in the perturbative treatment of gravitational instability (Bharadwaj 1996a). In both situations the scaling properties of the non-linear effects is determined by the pair velocity dispersion (Bharadwaj 1997) and at large scales the non-linear two-point correlation function can be interpreted in terms of the linear two-point correlation function modified by small scale random motions.

We now come back to the interpretation of equation (27). One of the main features is that it incorporates all the effects of the anisotropy and scale dependence of the pair velocity dispersion. As noted earlier, these two features arise because of the coherent flows. Whereas the convolution in equation (39) accounts only for the effects of random motions, the convolution with the distribution function in equation (27) also includes the effect of the coherent flows. The coherent flows reduce the width of the distribution function, causing a reduction in the elongation in  $\xi_s$ . The effect of the coherent flows is also present in the terms involving ratios of  $V_P$  and  $\sigma_P^2$ , the contribution of these terms increasing with the effect of coherent flows. All the terms involving  $V_P^2$  arise due to the non-linear redshift distortions.

In the linear analysis the redshift distortions produced by the coherent flows give rise to a flattening of the two-point correlation function along the line of sight. This effect is best captured by the quadrupole moment  $\xi_2$  which is predicted to be negative. The linear analysis also predicts a positive hexadecapole moment arising from the term involving the second derivative of  $\sigma_P^2(\mathbf{s})$  in equation (28) for  $\xi_s^L(\mathbf{s})$ .

Comparing our result with the predictions of the linear analysis of redshift distortions we see that the non-linear redshift space effects are more pronounced on the higher spherical moments  $\xi_l$  of the redshift space two-point correlation function. While the monopole  $\xi_0$  shows no significant deviations from the linear predictions, the deviations are around 10% on scales of  $10 - 20 h^{-1}\text{Mpc}$  for  $\xi_2$ . The moment  $\xi_4$  shows very large deviations from the linear predictions, the non-linear predictions differing by a factor of  $\sim 2$  on scales of  $10 - 20 h^{-1}\text{Mpc}$ .

A point which should be noted is that our analysis ignores all non-linear effect in the real space density fluctuations and peculiar velocities, and focuses only on the non-linear redshift distortions. While this assumption is expected to be valid for  $\xi_r$  and  $V_P$  at scales greater than  $10 h^{-1}\text{Mpc}$ , we do not expect this to hold for  $\sigma_P^2$  which has a constant isotropic part  $2\sigma^2$  arising from the random motions. This has a large contribution from small scales

which are non-linear and we do not expect the linear results used here to give a realistic estimate of  $\sigma_P^2$ . We also expect this effect to be present in our estimates on the effects on non-linear redshift distortions on the different angular moments of  $\xi_s$ . A possible solution is to use N-body simulations to determine the constant, isotropic part of  $\sigma_P^2$  and to use linear theory to calculate the contribution of the coherent flows. This possibility has not been explored here, and we plan to continue future work in this direction.

Another possibility which might arise but has not been taken into account is non-linear bias. A quadratic bias relation gives rise to two bias parameters  $b_1$  and  $b_2$ , and the relation between the fluctuations in the galaxy number density and the matter density is  $\delta_g = b_1\delta_m + \frac{1}{2}b_2\delta_m^2$ . In this situation  $\delta_g$  will no longer be a Gaussian random field and this will give rise to a new series of terms in equation (20) which could be summed up following the same procedure.

The effects of linear redshift distortion can be parametrized by a single parameter  $\beta = f(\Omega)/b$  and the analysis of redshift surveys based on this do not yield  $f(\Omega)$  and  $b$  separately. We find that  $\xi_4$ , the hexadecapole moment of  $\xi_s$ , depends on  $f(\Omega)$  and  $b$  separately when the non-linear effects of redshift distortions are taken into account. This holds the possibility of separately determining  $f(\Omega)$  and  $b$  from redshift surveys. Although this effect increases at small scales, the range  $10 - 20h^{-1}\text{Mpc}$  is possibly best suited for putting it to use. Non-linear effects in real space and non-linear biasing will become important at smaller scales. At these scales the hexadecapole moment is expected to be 10% of the quadrupole moment. Further investigations are needed to determine the range of validity of the results presented here before they can be applied to the analysis of redshift surveys.

## 5 Acknowledgements.

The author would like to thank Debaprasad Giri and Akhilesh Singh for their help while writing this paper. The author is also thankful to MRI, Allahabad for its hospitality during a part of the period when this was being completed.

## 6 Appendix A.

In this appendix we discuss, in some detail, the relation between  $\xi_r(r)$ ,  $V_P(\mathbf{r})$ ,  $\sigma_P^2(\mathbf{r})$  and  $\xi(r)$ . In the linear regime  $\delta(\mathbf{r}_1)$ , the fluctuation in the dark matter

density, can be expressed in terms of a potential  $\psi(\mathbf{r}_1)$  as

$$\delta(\mathbf{r}_1) = \nabla^2 \psi(\mathbf{r}_1), \quad (40)$$

and the peculiar velocity  $\mathbf{v}(\mathbf{r}_1)$  can be expressed as

$$\mathbf{v}(\mathbf{r}_1) = -f(\Omega) \nabla \psi(\mathbf{r}_1), \quad (41)$$

In addition, assuming a linear bias relation,  $\delta_g(\mathbf{r}_1)$  the fluctuation in the galaxy number density can be expressed as

$$\delta_g(\mathbf{r}_1) = b \nabla^2 \psi(\mathbf{r}_1). \quad (42)$$

Using these we can express  $\xi(r)$  as

$$\xi(r) = \langle \delta(\mathbf{r}_1) \delta(\mathbf{r}_2) \rangle = \langle \nabla^2 \psi(\mathbf{r}_1) \nabla^2 \psi(\mathbf{r}_2) \rangle = \nabla^4 \phi(r) \quad (43)$$

where  $\mathbf{r} = \mathbf{r}_2 - \mathbf{r}_1$  and  $\phi(r) = \langle \psi(\mathbf{r}_1) \psi(\mathbf{r}_2) \rangle$ . Equation (43) can be inverted to express  $\phi(r)$  and its derivatives in terms of  $\xi(r)$ .

We use these to calculate  $V_P(\mathbf{r})$ , which gives us

$$\begin{aligned} V_P(\mathbf{r}) &= \langle \mathbf{n} \cdot (\mathbf{v}(\mathbf{r}_2) - \mathbf{v}(\mathbf{r}_1)) (\delta_g(\mathbf{r}_2) + \delta(\mathbf{r}_1)) \rangle \\ &= (-bf) \langle \mathbf{n} \cdot (\nabla \psi(\mathbf{r}_2) - \nabla \psi(\mathbf{r}_1)) (\nabla^2 \psi(\mathbf{r}_2) + \nabla^2 \psi(\mathbf{r}_1)) \rangle \\ &= -2fb(\mathbf{n} \cdot \nabla) \nabla^2 \phi(r) \end{aligned} \quad (44)$$

This can be further simplified using equation (43) to obtain

$$\begin{aligned} V_P(\mathbf{r}) &= -2fb \frac{\partial}{\partial r_{\parallel}} (\nabla^2)^{-1} \xi(r) \\ &= -\frac{2bfr_{\parallel}}{3} \bar{\xi}_2(r) \end{aligned} \quad (45)$$

We next consider  $\sigma_P^2(\mathbf{r})$  which can be expressed as

$$\begin{aligned} \sigma_P^2(\mathbf{r}) &= \langle \mathbf{n} \cdot (\mathbf{v}(\mathbf{r}_2) - \mathbf{v}(\mathbf{r}_1)) \mathbf{n} \cdot (\mathbf{v}(\mathbf{r}_2) - \mathbf{v}(\mathbf{r}_1)) \rangle \\ &= -2f^2 \langle [\mathbf{n} \cdot \nabla \psi(\mathbf{r}_1)] [\mathbf{n} \cdot \nabla \psi(\mathbf{r}_2)] \rangle + \sigma^2 \\ &= 2f^2 \frac{\partial^2}{\partial r_{\parallel}^2} \phi(r) + \sigma^2 \end{aligned} \quad (46)$$

where  $\sigma^2 = \langle (\mathbf{n} \cdot \mathbf{v})^2 \rangle$  is the one dimensional peculiar velocity dispersion. The expression for  $\sigma_P^2(\mathbf{r})$  can be further simplified using (43) to obtain

$$\begin{aligned} \sigma_P^2(\mathbf{r}) &= 2f^2 \frac{\partial^2}{\partial r_{\parallel}^2} (\nabla^2)^{-2} \xi(r) + \sigma^2 \\ &= f^2 \left[ \frac{r^2}{3} \bar{\xi}_1(r) - \frac{r_{\perp}^2}{3} \bar{\xi}_2(r) + \frac{(r^2 - 3r_{\parallel}^2)}{15} \bar{\xi}_4(r) \right] \end{aligned} \quad (47)$$

## 7 Appendix B.

In this appendix we consider a limiting situation where the separation  $s$  at which the redshift two-point correlation is being calculated is very large. We also assume that the real space two-point correlation function is a power law  $\xi_r(s) \propto s^{-\gamma}$  with  $\gamma > 2$  at large separations. The power law requirement is not crucial and the arguments presented here are valid provided the integral  $\int_y^x \xi_r(s) s ds$  converges for  $x \rightarrow \infty$ .

With the power law assumption we have  $V_P(\mathbf{s}) \propto s^{1-\gamma}$  (eq. 45),  $\sigma_P^2(\mathbf{s}) - 2\sigma^2 \propto s^{2-\gamma}$  (eq. 47) and  $\sigma_P^2(\mathbf{s}) \simeq 2\sigma^2$  for large values of  $s$ . The point to note is that at large separations the correlation between the galaxy peculiar velocities is very small and the pair velocity dispersion is nearly isotropic and has a constant value  $2\sigma^2$ .

We next shift our attention to equation (20) which expresses  $\xi_s$  as a series of different terms involving  $\xi_r, V_P$  and  $\sigma_P^2$ . In the linear regime each of these quantities is characterized by a small number  $\epsilon \sim \delta\rho/\rho$  and  $\xi_r \sim V_P \sim \sigma_P^2 \sim \epsilon^2$ . Identifying all the terms of order  $\epsilon^{2m}$  in equation (20) we have

$$\begin{aligned} & \frac{1}{2^m m!} \frac{\partial^{2m}}{\partial s_{\parallel}^{2m}} [\sigma_P^2(\mathbf{s})]^m + \frac{1}{2^{m-1}(m-1)!} \frac{\partial^{2m-2}}{\partial s_{\parallel}^{2m-2}} [\sigma_P^2(\mathbf{s})]^{m-1} \xi_r(\mathbf{s}) \\ & + \frac{1}{2^{m-1}(m-1)!} \frac{\partial^{2m-1}}{\partial s_{\parallel}^{2m-1}} [\sigma_P^2(\mathbf{s})]^{m-1} V_P(\mathbf{s}) \\ & + \frac{1}{2^{m-2}(m-2)!} \frac{\partial^{2m-2}}{\partial s_{\parallel}^{2m-2}} [\sigma_P^2(\mathbf{s})]^{m-2} \frac{V_P^2(\mathbf{s})}{4} \sim \epsilon^{2m} \end{aligned} \quad (48)$$

This contains terms involving different powers of  $s$ . The terms whose  $s$  dependence is  $s^{2-\gamma-2m}$  fall off slowest with increasing  $s$  and these terms dominate at large separations. Retaining only these terms the above expression becomes

$$\frac{[\sigma^2]^{m-1}}{(m-1)!} \left[ \frac{1}{2} \frac{\partial^{2m}}{\partial s_{\parallel}^{2m}} \sigma_P^2(\mathbf{s}) + \frac{\partial^{2m-2}}{\partial s_{\parallel}^{2m-2}} \xi_r(\mathbf{s}) - \frac{\partial^{2m-1}}{\partial s_{\parallel}^{2m-1}} V_P(\mathbf{s}) \right] \quad (49)$$

Summing up all the terms with different powers of  $\epsilon^2$  we obtain

$$1 + \xi_s(\mathbf{s}) = 1 + \sum_{q=0}^{\infty} \frac{\sigma^{2q}}{q!} \frac{\partial^{2q}}{\partial s_{\parallel}^{2q}} \left[ \xi_r(\mathbf{s}) - \frac{\partial}{\partial s_{\parallel}} V_P(\mathbf{s}) + \frac{1}{2} \frac{\partial^2}{\partial s_{\parallel}^2} \sigma_P^2(\mathbf{s}) \right] \quad (50)$$

where the terms in the square bracket is the linear redshift two-point correlation function  $\xi_s^L(\mathbf{s})$  (equation 28). We next sum up all the terms following a procedure similar to that used in section 2 (equation 22 to 27) and obtain

$$\xi_s(s_{\perp}, s_{\parallel}) = \int ds'_{\parallel} G(s'_{\parallel}, \sqrt{2}\sigma) \xi_s^L(s_{\perp}, s_{\parallel} + s'_{\parallel}). \quad (51)$$

## References

- [1] Ballinger W.E., Peacock, J.A. & Heavens, A.F. 1996, MNRAS, 282, 877
- [2] Benson, A. J., Cole, S., Frenk, C. S., Baugh, C. M. & Lacey, C. G. 2000, ApJ, 311, 793
- [3] S Bharadwaj, ApJ, 1996a, 460, 28
- [4] Bharadwaj S., ApJ, 1996b, 472, 1
- [5] Bharadwaj S., ApJ, 1997, 477, 1
- [6] Bharadwaj S., ApJ, 1999, 516, 507
- [7] Brainerd T.G., Bromley B.C., Warren M.S. & Zurek W.H. 1996, ApJ, 464, L103
- [8] Bromley B.C., Warren M.S. & Zurek W.H. 1997, ApJ, 475, 414
- [9] Bunn E. F. & White M. 1996, astro-ph/9607060
- [10] Cen, R. & Ostriker J. P. 1992. ApJ, 399, L113
- [11] Dekel, A. & Lahav, O. 1999, ApJ, 520, 24
- [12] Dressler, A. 1980, ApJ, 236, 351
- [13] Efstathiou, G., Bond, J. R. & White, S. D. M. 1992, MNRAS, 250, 1p
- [14] Fisher K. B., Davis M., Strauss M. A., Yahil A. & Huchra J.P. 1994, MNRAS, 267, 927
- [15] Fisher K. B., Scharf C. A. & Lahav O. 1994, MNRAS, 266, 219
- [16] Fisher K.B. & Nusser A. 1996, MNRAS, 279L, 1
- [17] Gramman M., Cen R. & Bahcall N. A. 1993, ApJ, 419, 440
- [18] Guzzo, L., Strauss, M. A., Fisher, K. B., Giovanelli, R., & Haynes, M. P. 1997, ApJ, 489, 37
- [19] Hamilton A. J. S. 1992, ApJ, 385, L5
- [20] Hamilton A. J. S. & Culhane M. 1996, MNRAS, 278, 73

- [21] Hamilton A. J. S. 1998, in The Evolving Universe, ed. D. Hamilton (Dordrecht:Kluwer) 185
- [22] Hatton S.J. & Cole S. 1998, MNRAS, 296, 10
- [23] Heavens A. F. & Taylor A. N. 1995, MNRAS, 275, 483
- [24] Hermit, S., Santiago, B. X., Lahav, O., Strauss, M. A., Davis, M., Dressler, A., & Huchra, J. P. 1996, MNRAS, 283, 709
- [25] Hivon E., Bouchet F.R., Colombi S., & Juszkiewicz R. 1995, A&A, 298, 643
- [26] Hui L., Kofman L. & Shandarin S.F. 2000, 537, 12
- [27] Kaiser N. 1987, MNRAS, 227, 1
- [28] Kauffmann, G. Nusser, A. & Steinmetz, M. 1997, MNRAS, 286, 795
- [29] Lahav, O., Nemiroff, R. J., & Piran, T. 1990, ApJ, 350, 119
- [30] Loveday *et al.* 1995, ApJ, 442, 457
- [31] Mann, R. G., Peacock, J. A., Heavens, A. F. 1998, MNRAS, 293, 209
- [32] Peacock, J. A., *et al.* 2001, Nature, 410, 169
- [33] Peacock, J. A., & Dodds, S.J. 1994, MNRAS, 267, 1020
- [34] Peebles, P. J. E. 1990, The LArge-Scale Structure of the Universe, (Princeton: Princeton University Press)
- [35] Pen, U.-L. 1998, ApJ, 504, 601
- [36] Santiago, B. X. & Strauss, M. A. 1992, ApJ, 387, 9
- [37] Suto, Y. and Sugino, T. 1991, ApJL, 370, L15
- [38] Szalay, A.S., Matsubara, T. and Landy, S.D. 1998, ApJ, 498, L1.
- [39] Taruya, A., Magara, H., Jing, Y. P. & Suto, Y. 2001, PASJ, 53, 155
- [40] Taylor A. N. & Hamilton A. J. S. 1996, MNRAS, 282, 767
- [41] Zaroubi S. & Hoffman Y. 1996, 462, 25

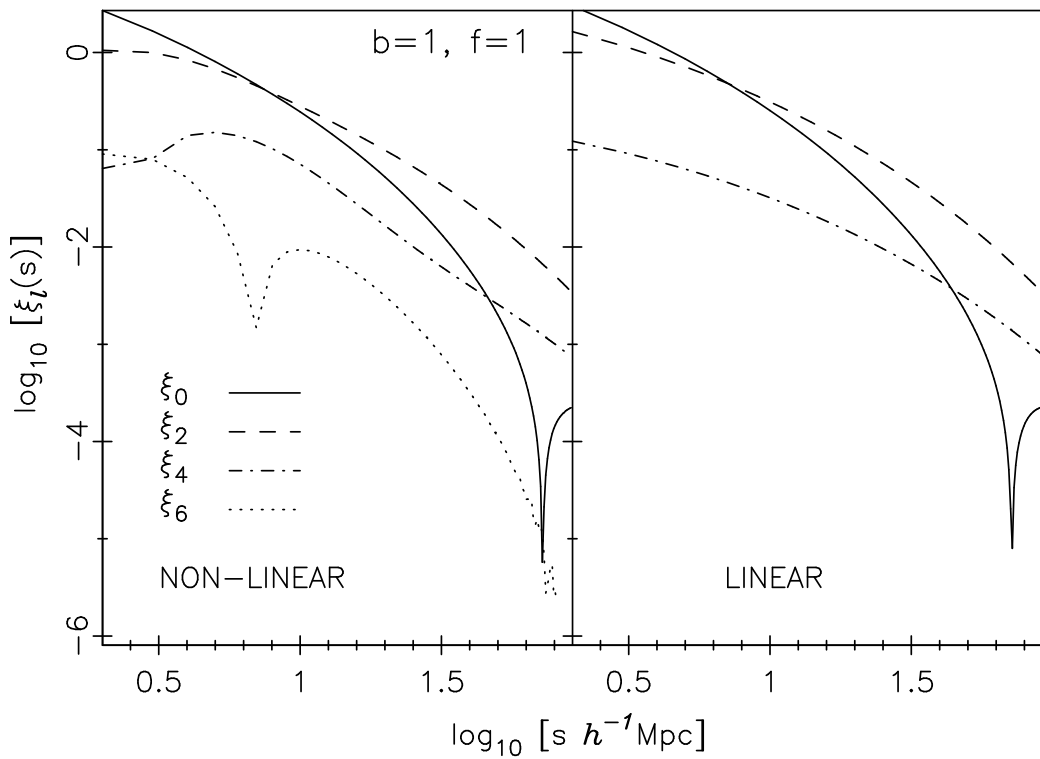


Figure 1: This shows  $\xi_l$ , the various spherical harmonics of the redshift space two-point correlation function calculated using eq. (27) (NON-LINEAR) and eqs. (35)-(37) (LINEAR) for a COBE normalised CDM power spectrum with  $\Gamma = 0.25$  and  $h = 0.5$ .

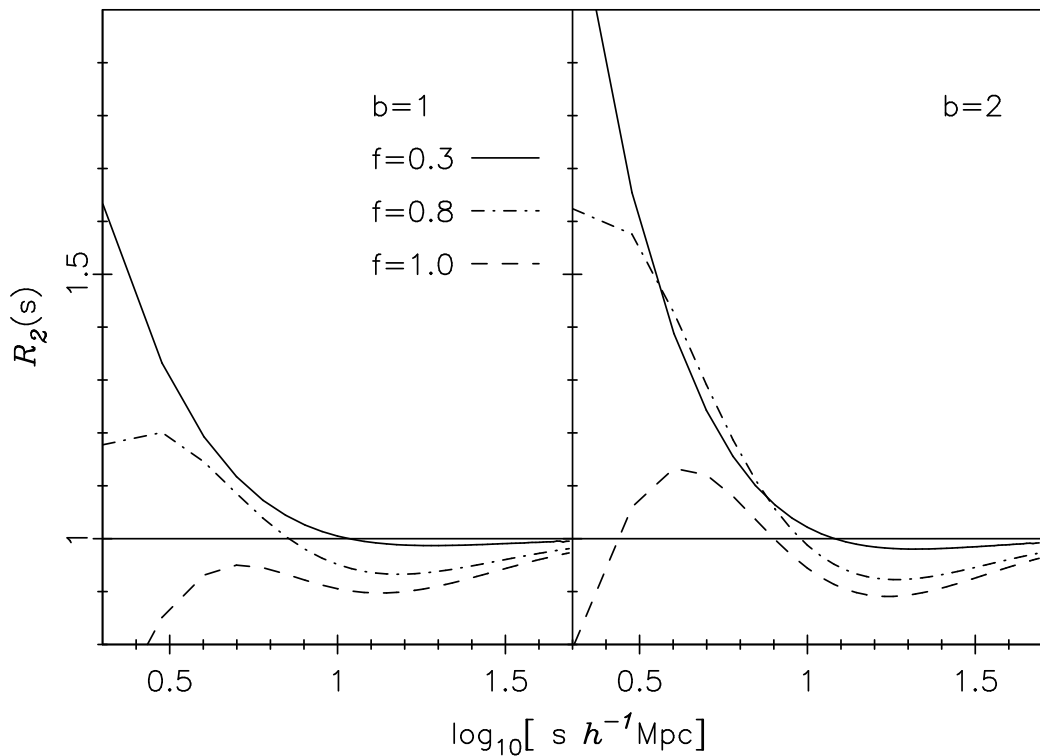


Figure 2: The plots show  $R_2 = \xi_2 / \xi_2^L$  for different values of  $f(\Omega)$  and  $b$  for a COBE normalised  $\Gamma = 0.25$ ,  $h = 0.5$  CDM power spectrum.

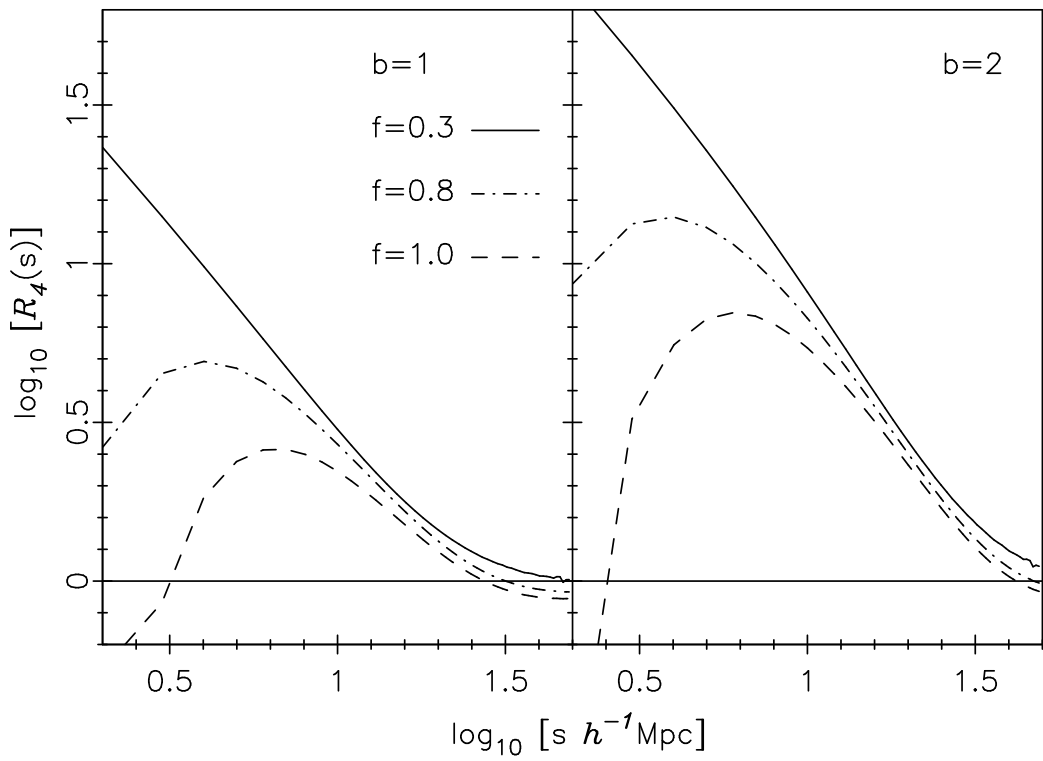


Figure 3: The plots show  $R_4 = \xi_4 / \xi_4^L$  for different values of  $f(\Omega)$  and  $b$  for a COBE normalised  $\Gamma = 0.25$ ,  $h = 0.5$  CDM power spectrum.

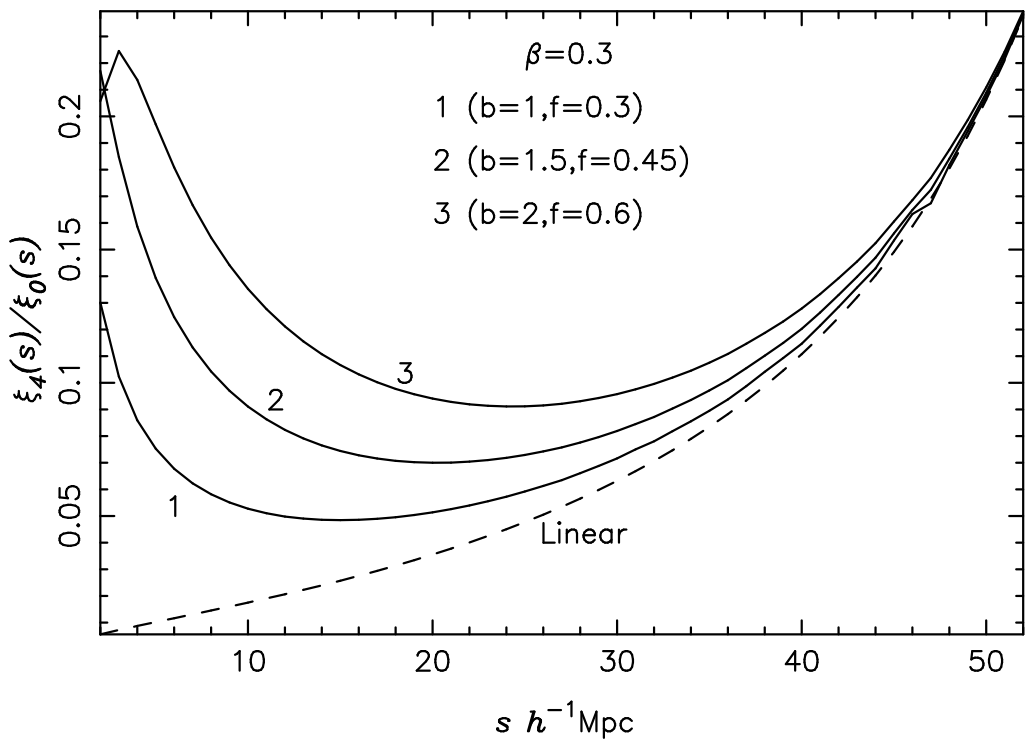


Figure 4: This shows  $\xi_4/\xi_0$  for different values of  $f(\Omega)$  and  $b$  all with  $\beta = f(\Omega)/b = 0.3$  for a COBE normalised  $\Gamma = 0.25$ ,  $h = 0.5$  CDM power spectrum.